

Fractional-order controllers for stick-slip vibration mitigation in oil well drill-strings

Journal of Low Frequency Noise,
Vibration and Active Control
2021, Vol. 40(3) 1571–1584
© The Author(s) 2021
DOI: 10.1177/1461348420984040
journals.sagepub.com/home/lfn



Massinissa Derbal¹, Mohamed Gharib² , Shady S Refaat¹,
Alan Palazzolo³ and Sadok Sassi⁴

Abstract

Drillstring–borehole interaction can produce severely damaging vibrations. An example is stick–slip vibration, which negatively affects drilling performance, tool integrity and completion time, and costs. Attempts to mitigate stick–slip vibration typically use passive means and/or change the operation parameters, such as weight on bit and rotational speed. Automating the latter approach, by means of feedback control, holds the promise of quicker and more effective mitigation. The present work presents three separate fractional-order controllers for mitigating drillstring slip–stick vibrations. For the sake of illustration, the drillstring is represented by a torsional vibration lumped parameter model with four degrees of freedom, including parameter uncertainty. The robustness of these fractional-order controllers is compared with traditional proportional-integral-derivative controllers under variation of the weight on bit and the drill bit’s desired rotary speed. The results confirm the proposed controllers effectiveness and feasibility, with rapid time response and less overshoot than conventional proportional-integral-derivative controllers.

Keywords

Drillstring dynamics, stick–slip, torsional vibration, mathematical modeling, fractional-order control

Introduction

The drillstring system plays a vital role in the oil and gas extraction industry by transferring torque and weight on bit (WOB) from the rotary table on the surface to the bit in the borehole. A drillstring consists of four major parts, including a rotary table, slender drill pipes, drill collars, and a drill bit. The drillstring can extend several kilometers deep, with a diameter not exceeding 30 cm.¹ This relatively long, thin structure is susceptible to severe vibrations that can lead to a reduced penetration rate, drill bit wear, and string failure. Drillstring vibration is generally classified into three types: axial, lateral, and torsional.² Torsional stick–slip vibration is generally severe and can lead to mechanical failure of drilling tools, extend drilling time, raise the drilling operations’ cost, and endanger workers.³ The primary indicator of stick–slip is a large difference between the top drive’s constant velocity and the bit’s angular velocity, which may vary between zero (stick) and up to six times the top drive’s velocity (slip).

¹Electrical Engineering Department, National Polytechnic School, Algiers, Algeria

²Mechanical Engineering Department, Texas A&M University at Qatar, Doha, Qatar

³Mechanical Engineering Department, Texas A&M University, College Station, TX, USA

⁴Mechanical and Industrial Engineering Department, Qatar University, Doha, Qatar

Corresponding author:

Mohamed Gharib, Mechanical Engineering Department, Texas A&M University at Qatar, Doha, Qatar.

Email: mohamed.gharib@qatar.tamu.edu



Recent research studies have modeled drillstrings' stick-slip vibrations, including control systems,³⁻⁵ which use low-order models as required by the control laws considered.⁶ Challamel⁷ used a simple torsional-axial dynamic model to demonstrate stick-slip vibration control, with limited instability in the stationary solution. Good agreement was shown in an experimental-theoretical correlation study of a dynamically coupled motor and drillstring in Vaziri et al.⁸ The bottom hole assembly (BHA) inertia was represented as a "flywheel" oscillator with a single degree of freedom (DOF) in Rudat et al.⁹; Qiu et al.¹⁰; Lin and Wang¹¹; Canudas de Wit et al.¹²; and Zhu et al.¹³; however, stick-slip motion was not simulated. A drillstring model with a constant rotary speed and 2-DOF was analyzed in Zhang and Xv³ and Canudas de Wit et al.¹² The present work uses a more general 4-DOF model, which considers the dynamics of the drill pipe and the drill collars. The bit-rock interaction is represented by dry friction, combined with a decaying exponential law.⁶

Various control techniques have been proposed to mitigate stick-slip torsional vibrations. Vibration control of a drillstring demands the flexibility to accommodate many operating conditions and the effectiveness needed for a complex drillstring dynamics plant.¹ Passive control approaches generally involve structural modifications to the drillstring,¹³ such as the design and optimization of the BHA's configuration, the selection of the drill bit,¹⁴ and implementation of anti-stick-slip tools in the BHA for drilling optimization.^{15,16} In contrast, active control approaches use an actuation mechanism guided by feedback signals related to the actual drill bit's velocity and angular position. Many active control techniques have been proposed, such as the introduction of a soft torque rotary system at the top to create a vibration absorber,¹⁷ and the adoption of a classical proportional-integral-derivative (PID) controller.¹⁸ More advanced techniques have been simulated, such as H-infinity (H_∞) control and linear quadratic control.^{19,20}

Fractional-order proportional-integral-derivative (FOPID) controllers were introduced in 1994.²¹ They have more parameters to tune to adjust the controlled system than classical PID controllers. They also provide more space to design the controller precisely and more accurately to fit the control requirements. Many engineers and scientists have adopted such controllers to achieve the highest stability of control by using different designs and tuning methods.^{22,23} Zhang and Xv³ designed a new FOPID for suppressing the stick-slip vibration of a drill string system. However, their research did not study dynamic performance under the variation of WOB and reference velocity. However, their research did not study the dynamic performance under the variation of the WOB and the reference velocity. Furthermore, their results were not compared with existing work in the literature.

The main contribution of the present work is the design of two novel fractional-order proportional-integral (FOPI) and fractional-order proportional-derivative (FOPD) controllers, and to implement them with a newly developed FOPID controller for stick-slip vibration mitigation. Specific fractional-order controller topics covered include: (i) the development of mathematical models for FOPI and FOPD, which represent generalized forms of a conventional proportional derivative (PI), and a conventional proportional derivative (PD) controller as discussed by Lin et al.¹; (ii) a study of the dynamic performance of the three fractional-order controllers under variation of the WOB and reference velocity; and (iii) a comparison of fractional order vs. conventional PID controllers.

Applying the proposed control method to drillstring vibration mitigation is a novel application (e.g. Zhao et al.²⁴). The drillstring is a complex system including an electric motor that rotates the rotary table, coupled with drill pipes and drill collars, and finally the drill bit. The bit-rock interaction and drilling mud-related forces introduce complicated, nonlinear terms into the plant model, and increase the difficulty of control.

This paper is structured as follows: A lumped-parameter, 4-DOF model for the drillstring with bit-rock interaction is presented in Section "Modeling of the drillstring system". The proposed control strategy is discussed, and the designs of the FOPI, FOPD, and FOPID controllers are presented in Section "Modeling and design of the fractional controllers". The simulation results are discussed in Section "Simulation results and discussion". Finally, the main conclusions are presented in Section "Conclusion".

Modeling of the drillstring system

During the drilling process, the power system drives the rotary table to move the drillstring into the well by the kelly, causing the drillstring to rotate with the drill bit. Figure 1 shows a torsional model of a drillstring. The model is composed of four elements: the top rotary system, the drill pipes, the drill collars, and the drill bit. Their inertias are, respectively J_r , J_p , J_c , and J_b . They are connected by linear springs with torsional damping (C_t , C_{tb} ,

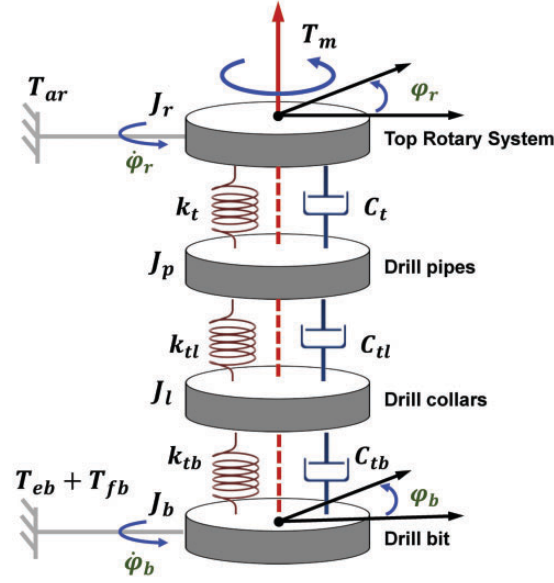


Figure 1. Torsional model of drillstring.

C_{tb}) and torsional stiffness (k_t, k_{tl}, k_{tb}), where T_{eb} is a viscous damping torque considered at the top drive system, and T_{fb} is a dry friction torque considered at the bit.

The equations of motion for the system shown in Figure 1 can be written as⁶

$$\begin{aligned}
 \ddot{\varphi}_r &= -\frac{C_t}{J_r}(\dot{\varphi}_r - \dot{\varphi}_p) - \frac{k_t}{J_r}(\varphi_r - \varphi_p) + \frac{T_m - T_{ar}}{J_r} \\
 \ddot{\varphi}_p &= \frac{C_t}{J_p}(\dot{\varphi}_r - \dot{\varphi}_p) + \frac{k_t}{J_p}(\varphi_r - \varphi_p) - \frac{C_{tl}}{J_p}(\dot{\varphi}_p - \dot{\varphi}_l) \\
 &\quad - \frac{k_{tl}}{J_p}(\varphi_p - \varphi_l) \\
 \ddot{\varphi}_l &= \frac{C_{tl}}{J_l}(\dot{\varphi}_p - \dot{\varphi}_l) + \frac{k_{tl}}{J_l}(\varphi_p - \varphi_l) - \frac{C_{tb}}{J_l}(\dot{\varphi}_l - \dot{\varphi}_b) \\
 &\quad - \frac{k_{tb}}{J_l}(\varphi_l - \varphi_b) \\
 \ddot{\varphi}_b &= \frac{C_{tb}}{J_b}(\dot{\varphi}_l - \dot{\varphi}_b) + \frac{k_{tb}}{J_b}(\varphi_l - \varphi_b) + \frac{T_{ab} + T_{fb}}{J_b}
 \end{aligned} \tag{1}$$

where $\dot{\varphi}_i$ and φ_i ($i \in r, p, l, b$) are the velocities and the angular displacements of drillstring elements, respectively; $T_m = u$ is the electrical motor torque; u is the control input; $T_{ar} = C_r \dot{\varphi}_r$ is the viscous damping torque of the top rotating system, and C_r is the viscous damping coefficient. The friction torque T_{fb} on the drill bit is given by Navarro-López and Cortés⁶

$$T_{fb} = \begin{cases} T_{eb} & \text{if } |\dot{\varphi}_b| < \xi, |T_{eb}| \leq T_{sb} \\ T_{sb} \text{sign}(T_{eb}) & \text{if } |\dot{\varphi}_b| < \xi, |T_{eb}| > T_{sb} \\ \text{WOB } R_b \mu_b \text{sign}(\dot{\varphi}_b) & \text{if } |\dot{\varphi}_b| \geq \xi \end{cases} \tag{2}$$

where T_{eb} is the torque applied to the drill bit⁶ and is expressed by

$$T_{eb} = C_{tb}(\dot{\varphi}_l - \dot{\varphi}_b) + k_{tb}(\varphi_l - \varphi_b) - T_{ab} \tag{3}$$

where $\xi > 0$ specifies a small enough neighborhood of $\dot{\varphi}_b = 0$, T_{sb} is the maximum static friction torque between the drill bit and the rock, $T_{sb} = WOB R_b \mu_{sb}$, WOB is the weight on bit, R_b is the bit radius, and μ_b is the dry friction coefficient given by Navarro-López and Cortés⁶

$$\mu_b = \mu_{cb} + (\mu_{sb} - \mu_{cb}) \text{Exp}[-\gamma_b |\varphi_b|]; 0 < \gamma_b < 1 \quad (4)$$

where μ_{sb} is the drill bit's static friction coefficient and μ_{cb} is the Coulomb friction coefficient. The system state vector³ can be defined as

$$\begin{aligned} \mathbf{x} &= (\dot{\varphi}_r, \varphi_r - \varphi_p, \dot{\varphi}_b, \varphi_b - \varphi_l, \dot{\varphi}_l, \varphi_l - \varphi_b, \dot{\varphi}_b)^T \\ \mathbf{x} &= (x_1, x_2, x_3, x_4, x_5, x_6, x_7)^T \end{aligned} \quad (5)$$

This system is a seventh-order nonlinear system. The bit-rock interaction causes complex response characteristics.

$$\begin{aligned} \dot{x}_1 &= \frac{1}{J_r} [-(C_t + C_r) x_1 - k_t x_2 + C_t x_3 + u] \\ \dot{x}_2 &= x_1 - x_3 \\ \dot{x}_3 &= \frac{1}{J_p} [C_t x_1 + k_t x_2 - (C_t + C_{tl}) x_3 - k_{tl} x_4 + C_{tl} x_5] \\ \dot{x}_4 &= x_3 - x_5 \\ \dot{x}_5 &= \frac{1}{J_l} [C_{tl} x_3 + k_{tl} x_4 - (C_{tl} + C_{tb}) x_5 - k_{tb} x_6 + C_{tb} x_7] \\ \dot{x}_6 &= x_5 - x_7 \\ \dot{x}_7 &= \frac{1}{J_b} [C_{tb} x_5 + k_{tb} x_6 - (C_{tb} + C_b) x_7 - T_{fb}] \end{aligned} \quad (6)$$

where the input of the state equation obtained by equation (6) is

$$u = C_t(x_1 - x_3) + k_t x_2 + C_r x_1 \quad (7)$$

Modeling and design of the fractional controllers

In this section, the definition of fractional calculus adopted with its approximation method is introduced. Also, the general transfer function of fractional-order transfer functions and the designed FOPI, FOPD, and FOPID models are presented. The fractional calculus principle is used to deal with real orders for the integral and derivative operators instead of integer orders. Multiple definitions of the fractional-order derivative have been presented in the literature, such as Riemann–Liouville, Grunwald–Letnikov, and M. Caputo's definitions.^{25–28} The fractional-order derivative of a function $f(t)$ is denoted by ${}_a D_t^\alpha$. The Riemann–Liouville definition is given by Petráš²⁵

$${}_a D_t^\alpha = \frac{1}{\Gamma(n - \alpha)} \frac{d^n}{dt^n} \int_a^t \frac{f(\tau)}{(t - \tau)^{\alpha - n + 1}} d\tau \quad (8)$$

Alternatively, the Grunwald–Letnikov definition is given by Loverro²⁶

$${}_a D_t^\alpha = \lim_{n \rightarrow 0} \frac{1}{h^\alpha} \sum_{j=0}^{\lfloor \frac{t-a}{h} \rfloor} (-1)^j \binom{\alpha}{j} f(t - jh) \quad (9)$$

where $\lfloor (t - a)/h \rfloor$ means the integer part and h is the time increment, where

$$\binom{\alpha}{j} = \frac{\Gamma(n + \alpha)}{\Gamma(j + 1)\Gamma(\alpha - j + 1)} \quad (10)$$

In this paper, the definition of Caputo fractional-order derivatives²⁸ has been adopted because it is popular in engineering applications.²⁹ The Caputo fractional-order derivative of a function $f(t)$, denoted ${}_aD_t^\alpha$, is described as^{27,28}

$${}_aD_t^\alpha = \frac{1}{\Gamma(n - \alpha)} \int_a^t \frac{f^n(\tau)}{(1 - \tau)^{\alpha-n+1}} d\tau \tag{11}$$

where α is a real number, n is an integer that satisfies the condition $(n - 1 \leq \alpha < n)$, a and t are the limits of integration, and Γ is the Gamma function.³⁰ Other recent definitions were introduced, such as two-scale fractal derivative^{31,32} and He's fractional derivative^{33,34} definitions. The two-scale fractal derivative is given by He and Ain³¹ and Ain and He³²

$$\frac{df(t)}{dt^\alpha} = \Gamma(n + \alpha) \lim_{t \rightarrow t_0} \frac{f(t) - f_0(t)}{(t - t_0)^\alpha} \tag{12}$$

where α is the two-scale dimension. The He's definition based on the variational iteration method given by^{33,34}

$${}_aD_t^\alpha = \frac{1}{\Gamma(n - \alpha)} \frac{d^n}{dt^n} \int_{t_0}^t (s - t)^{\alpha-n-1} [f_0(s) - f(s)] ds \tag{13}$$

where $f_0(t)$ is a known function

Most fractional-order differential equations do not have exact analytic solutions because of the complexity of the fractional calculus, therefore many numerical and analytical methods have been proposed to determine approximate solutions.^{35,36}

Oustaloup's recursive approximation has been adopted in this work because this method has been widely used to describe fractional-order systems with the use of integer order.^{37,38} It can be applied within a specified frequency range $[\omega_l, \omega_h]$, between the boundaries of the low cut-off and high cut-off frequencies. This function³⁹ is given as follows

$$S^\alpha \approx k \prod_{n=1}^N \frac{1 + \frac{s}{\omega_{zn}}}{1 + \frac{s}{\omega_{pn}}} ; \alpha > 0 \tag{14}$$

where the gain k is adjusted to have unity gain at 1 rad/s, and N is the number of poles and zeros. The frequencies of the poles and zeros are given by the following recursive equations⁴⁰

$$\begin{aligned} \omega_{z,1} &= \omega_1 \sqrt{\eta} \\ \omega_{zn} &= \omega_{p,n-1} \eta; n = 1 \dots N \\ \omega_{pn} &= \omega_{z,n-1} \alpha; n = 1 \dots N \end{aligned} \tag{15}$$

where

$$\begin{aligned} \alpha &= \left(\frac{\omega_h}{\omega_l}\right)^{\frac{q}{N}} \\ \eta &= \left(\frac{\omega_h}{\omega_l}\right)^{\frac{1-q}{N}} \end{aligned} \tag{16}$$

The FOPID controller's generalized transfer function⁴¹ is given by

$$C(s) = \frac{U(s)}{E(s)} = K_p + \frac{K_I}{S^\lambda} + K_D S^\mu; \quad \lambda \geq 0 \quad \text{and} \quad \mu \geq 0 \tag{17}$$

where $U(s)$ is the control signal, $C(s)$ is the controller output, $E(s)$ is the error signal, μ is the order of differentiation, λ is the order of integration, K_I is the integration constant gain, K_P is the proportional constant gain, and

K_D is the derivative constant gain. The FOPID controller becomes a FOPI controller if the differential element is equal to zero. In that case, the FOPI controller transfer function is given as

$$C(s) = \frac{U(S)}{E(S)} = K_P + \frac{K_I}{S^\lambda}; \quad \lambda \geq 0 \quad (18)$$

The FOPID controller becomes a FOPD controller if the integral element n is equal to zero. In that case, the FOPD controller transfer function is given by

$$C(s) = \frac{U(S)}{E(S)} = K_P + K_D S^\mu; \quad \mu \geq 0 \quad (19)$$

The conventional PID controller is a particular case of the fractional-order controller, where λ and μ are equal to one; in this case, the PID controller transfer function can be written as

$$C(s) = \frac{U(S)}{E(S)} = K_P + \frac{K_I}{S} + K_D S \quad (20)$$

To mitigate the stick–slip vibration of the drillstring, FOPI, FOPD, and FOPID controllers are designed and implemented for the system in equation (6), and their transfer functions are given in equations (16) to (18), respectively

$$C(s) = \frac{K_{11}(\Omega - x_1)}{S^\lambda} + K_{12}(\Omega - x_1) + K_{13}(x_7 - x_1); \lambda \geq 0 \quad (21)$$

where Ω is the reference velocity, and K_{11} , K_{12} , and K_{13} represent the control gains of the proposed FOPI controller.

$$C(s) = K_{21}(\Omega - x_1) + K_{22}(\Omega - x_7)S^\mu + K_{23}(x_7 - x_1); \quad \mu \geq 0 \quad (22)$$

where K_{21} , K_{22} , and K_{23} represent the control gains of the proposed FOPD controller.

$$C(s) = \frac{K_{31}(\Omega - x_1)}{S^\lambda} + K_{32}(\Omega - x_7)S^\mu + K_{33}(x_7 - x_1); \quad \lambda \geq 0 \quad \text{and} \quad \mu \geq 0 \quad (23)$$

where K_{31} , K_{32} , and K_{33} represent the control gains of the proposed FOPID controller.

Simulation results and discussion

An extensive series of simulation studies on the control of the drillstring system was carried out in MATLAB/SIMULINK to verify the performance of the proposed controllers. The results of the torsional model of the drillstring were calculated with the system parameters in Table 1. The simulation results are given and discussed for both an uncontrolled and a controlled system with different types of fractional controller. An open system simulation was conducted to validate the theoretical analysis.

Open loop system simulation

The simulation results for equation (6) are shown in Figure 2, where the input u was kept constant at 100 kN.m. The reference velocity value is $\Omega = 12$ rad/s, which is a typical value for drilling operations.

Figure 2 shows that the drillstring system experiences significant stick–slip vibration. The rotary table, the drill pipe, the drill collar, and the drill bit all vibrate periodically. The stick–slip vibration at the drill bit is severe, and the viscous state and the sliding state are visible. The vibrations obtained for the drill pipe and drill collars associated with the stick–slip bit motion are in line with real drilling operations. Thus, the model in equation

Table 1. Numerical values for the drillstring system’s parameters.

Parameter	Symbol	Value	Units
Inertia of the rotary table	J_r	930	kg.m ²
Inertia of the drill pipe	J_p	2782.25	kg.m ²
Inertia of the drill collar	J_l	750	kg.m ²
Inertia of the drill bit	J_b	471.9698	kg.m ²
Torsional stiffness between the rotary table and the drill pipe	k_t	698.069	N.m/rad
Torsional stiffness between the drill pipe and the bottom hole assembly (BHA)	k_{tl}	1080	N.m/rad
Torsional stiffness between the BHA and the drill bit	k_{tb}	907.48	N.m/rad
Torsional damping between the rotary table and the drill pipe	C_{rd}	139,6126	N.m.s/rad
Torsional damping between the drill pipe and the BHA	C_{tl}	190	N.m.s/rad
Torsional damping between the BHA and the drill bit	C_{tb}	181.49	N.m.s/rad
Viscous damping coefficient of the rotary table	C_r	425	N.m.s/rad
Viscous damping coefficient of the drill bit	C_b	50	N.m.s/rad
Weight on bit	WOB	100	kN
Given speed	Ω	12	rad/s
Radius of the drill bit	R_b	0.155575	m
Coulomb friction coefficient	μ_{cb}	0.5	–
Static friction coefficient	μ_{sb}	0.8	–
A small enough neighborhood of $\dot{\varphi}_b = 0$	ξ	10^{-6}	–
Velocity decrease rate	γ_b	0.9	–

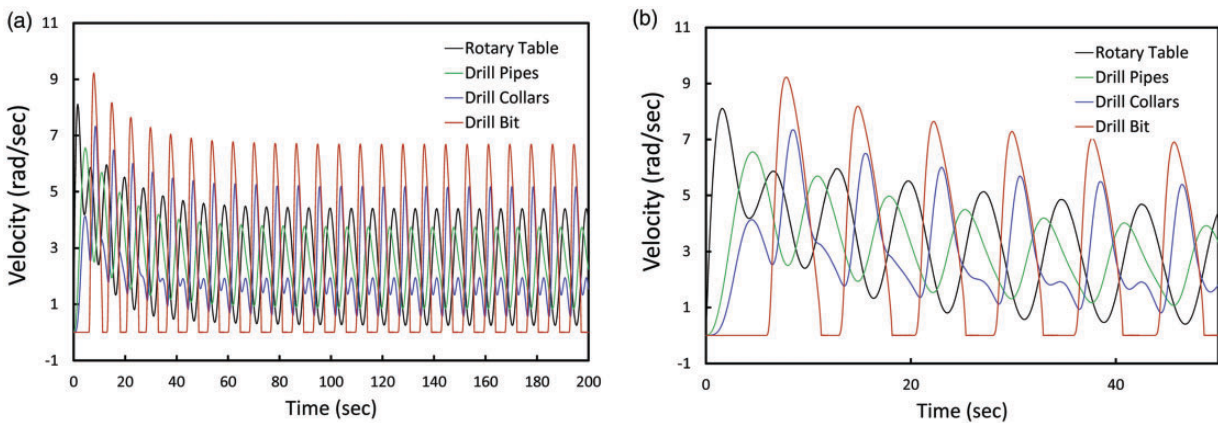


Figure 2. The angular velocity time response for drillstring stick–slip phenomena: (a) full range and (b) zoomed range.

(6) correctly describes stick–slip vibrations. This alignment with reality also proves the validity of the adopted lumped-parameter torsional model. Control of the drillstring system is needed to mitigate stick–slip vibrations and to protect the drilling tools.

Controlled systems

The designed FOPD, FOPI, and FOPID controllers were implemented for the first time in the drillstring system to mitigate the problem of stick–slip vibration; the results are compared with a traditional PID controller. The controllers’ robustness is evaluated under the variation of the WOB and the reference velocity. MATLAB’s FOMCON toolbox based on Oustaloup’s recursive approximation was used to simulate the fractional-order calculus.⁴²

The simulation was carried out under a constant WOB of 100 kN and $\Omega = 12$ rad/s, a typical value for drilling operations.

Figure 3 shows the results for rotary table velocity of the controlled drillstring system with the PID, FOPD, FOPI, and FOPID controllers. All the controllers can suppress the stick–slip vibration of the drillstring system at

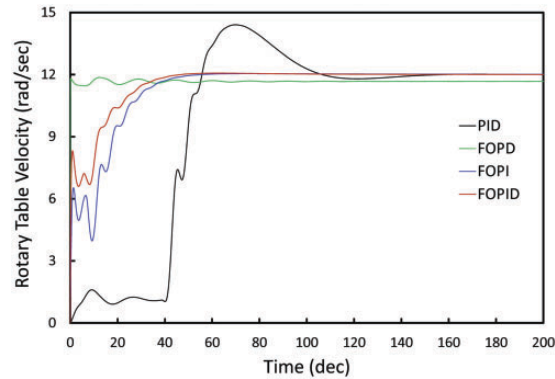


Figure 3. Controlled rotary table velocity.

PID: proportional-integral-derivative; FOPD: fractional-order proportional-derivative; FOPI: fractional-order proportional-integral; FOPID: fractional-order proportional-integral-derivative.

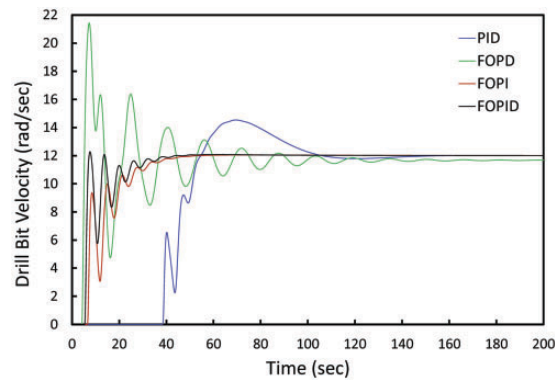


Figure 4. Controlled drill bit velocity.

PID: proportional-integral-derivative; FOPD: fractional-order proportional-derivative; FOPI: fractional-order proportional-integral; FOPID: fractional-order proportional-integral-derivative.

the surface. The FOPD controller has a faster response time (45 s), which can be explained by the absence of the integral parameter, which reduces the rise time in the control position.

However, due to the removal of the integrator, the FOPD controller stabilized at 11.67 rad/s, which is under the reference velocity value 12 rad/s. The FOPID has a faster response time than the FOPI and PID controllers, at 47, 55, and 160 s, respectively. The FOPD, FOPI, and FOPID controllers did not show any overshoots compared with the PID.

Figure 4 shows the drill bit velocities resulting from the controlled drillstring system with the proposed controllers. All the controllers can suppress the stick–slip vibration of the drillstring system at the bit. The FOPD controller has high oscillations with a peak neighboring 21.43 rad/s, which represents an overshoot of 78.58%. This overshoot results in a slower response time (182 s) caused by the FOPD's velocity control limits. The response stabilized under the reference velocity value of 11.67 rad/s instead of 12 rad/s because of the FOPD's steady-state error. The FOPID has a faster response time than the FOPI and PID at 48, 55, and 160 s, respectively. The FOPI and FOPID controllers did not show an overshoot compared with the PID.

Figure 5 shows the output control signals of the chosen controllers. The FOPD controller shows high oscillation with high overshoot (67.73%) because it is sensitive to disturbances in speed control. It has a slower response time (185 s) and it stabilizes at 13.1 kN.m instead of 13.28 kN.m, as seen for the other controllers. The FOPID has a faster response time than the FOPI and PID at 28, 35, and 140 s, respectively. However, the FOPI shows a lower overshoot (33.46 kN.m) than the FOPID and the PID (12.95 kN.m and 14.08 kN.m, respectively).

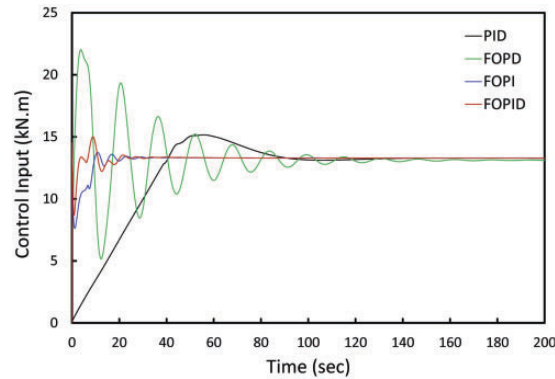


Figure 5. The control signals.

PID: proportional-integral-derivative; FOPD: fractional-order proportional-derivative; FOPI: fractional-order proportional-integral; FOPID: fractional-order proportional-integral-derivative.

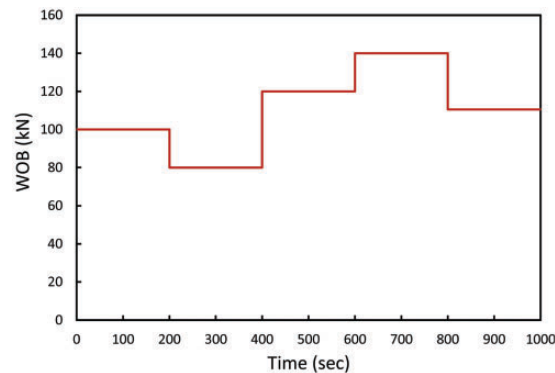


Figure 6. Variation in the weight on bit (WOB).

Variations in WOB. The controllers were evaluated under variation of the WOB, as shown in Figure 6, to evaluate their robustness. The WOB changed every 200 s by increasing and decreasing to 100, 80, 120, 140, and 110 kN. The reference velocity remained constant at 12 rad/s in this experiment.

Figure 7 shows the rotary table velocity results of the controlled drillstring system with PID, FOPD, FOPI, and FOPID controllers to demonstrate their response at the moment of WOB variation. All controllers could suppress the stick–slip vibration of the drillstring on the surface even under variation of the WOB. The FOPD had a faster response with no overshoot, which can be explained by the absence of the integral parameter, which reduces the rise time in the control position. The FOPD was slightly affected by the variation of the WOB, and it remains almost stable. The FOPID has a faster response time and a slower overshoot than the FOPI, which shows better performance than the PID.

Figure 8 shows the drill bit velocity response to WOB variation. The curves show the results of the drillstring system with PID, FOPD, FOPI, and FOPID controllers, respectively. All controllers suppressed the stick–slip vibration of the drillstring at the drill bit even under variation of the WOB. The FOPD has a slower response time with high oscillation. It is strongly affected by variation in the WOB as a result of the FOPD's velocity control limits. Moreover, the FOPID has a faster response time than the FOPI, which shows excellent performance compared with the PID.

Figure 9 shows the zoomed output control signals of the proposed controllers to demonstrate their response at the moment of WOB variation. The FOPD controller shows high oscillation with a high overshoot. It has a slower response time, and it is highly affected by the variation of the WOB as a result of the FOPD's velocity control limits. The FOPID controller has a faster response time than the FOPI and PID, and it has a smaller overshoot than the PID. However, the FOPI controller has no overshoot and a faster response time than PID under the WOB variation.

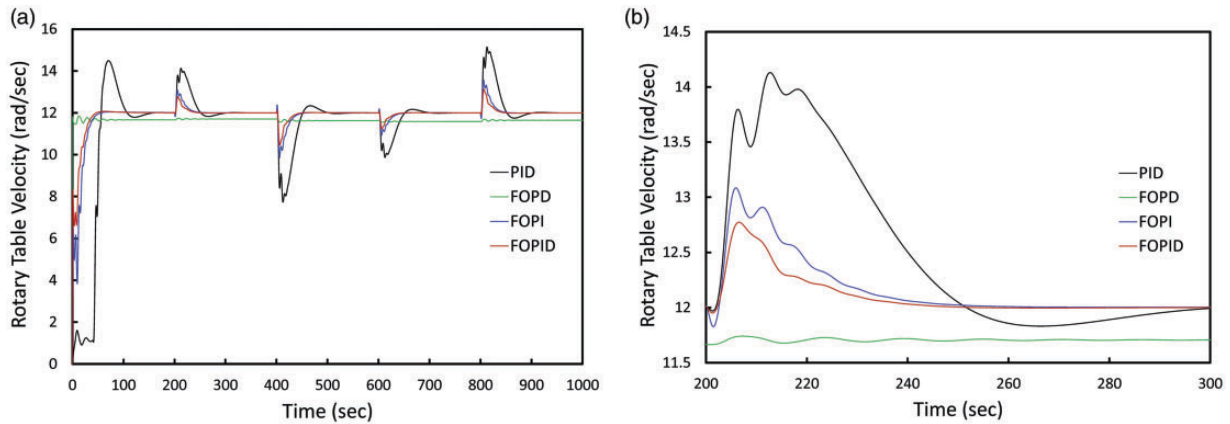


Figure 7. Rotary table velocities under variation of the weight on bit (WOB): (a) full range and (b) zoomed range. PID: proportional-integral-derivative; FOPD: fractional-order proportional-derivative; FOPI: fractional-order proportional-integral; FOPID: fractional-order proportional-integral-derivative.

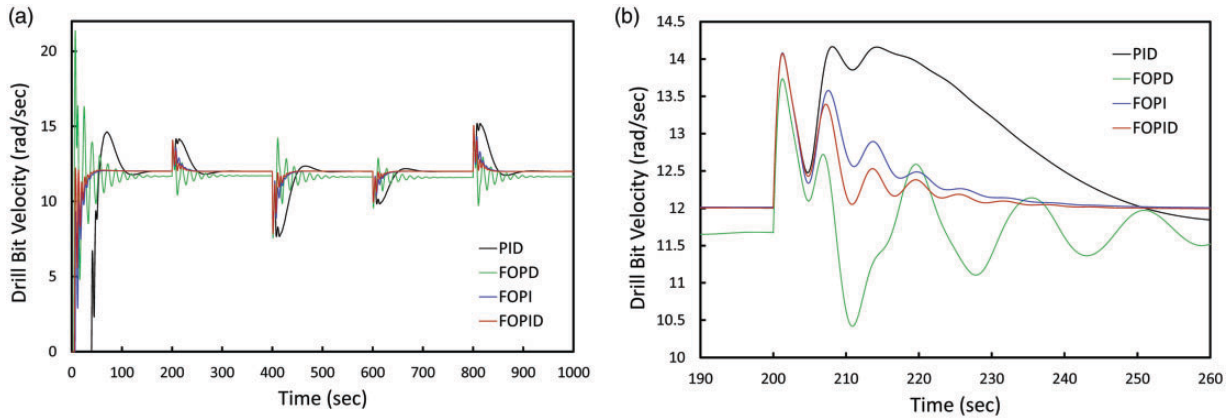


Figure 8. Drill bit velocities under variation of the weight on bit (WOB): (a) full range and (b) zoomed range. PID: proportional-integral-derivative; FOPD: fractional-order proportional-derivative; FOPI: fractional-order proportional-integral; FOPID: fractional-order proportional-integral-derivative.

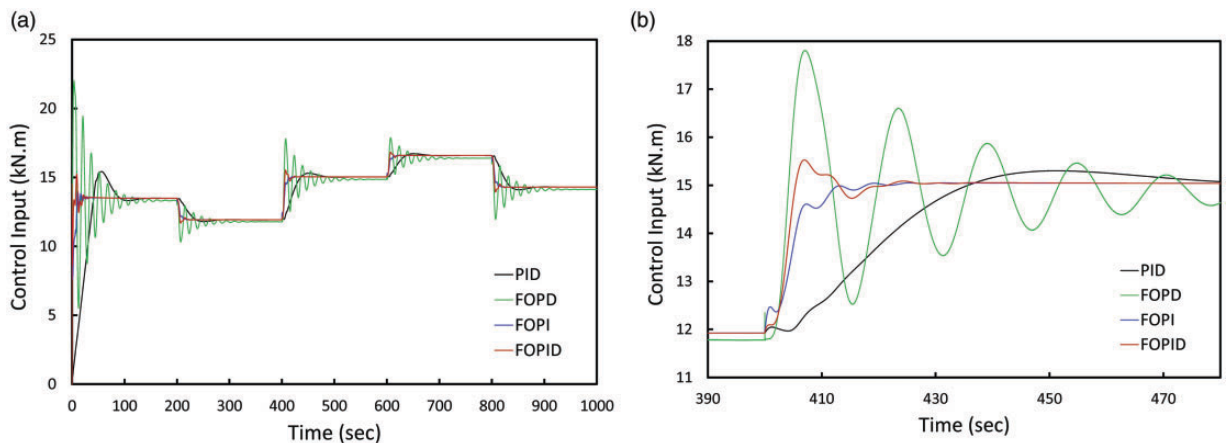


Figure 9. Control signals under WOB variation: (a) full range and (b) zoomed range. PID: proportional-integral-derivative; FOPD: fractional-order proportional-derivative; FOPI: fractional-order proportional-integral; FOPID: fractional-order proportional-integral-derivative.

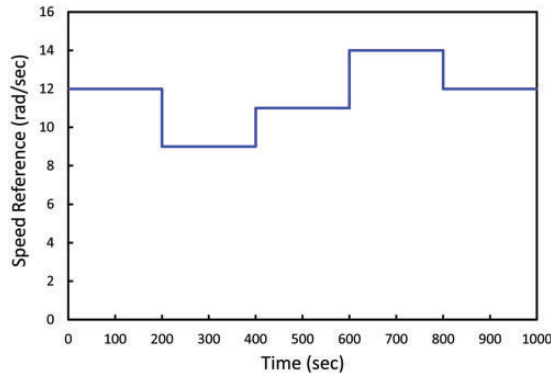


Figure 10. Variation in the reference velocity.

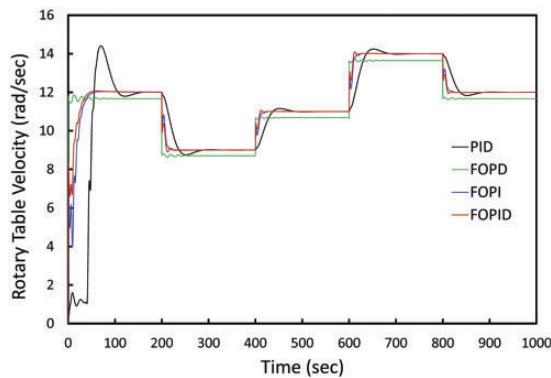


Figure 11. Rotary table velocities under variation of the velocity.

PID: proportional-integral-derivative; FOPD: fractional-order proportional-derivative; FOPI: fractional-order proportional-integral; FOPID: fractional-order proportional-integral-derivative.

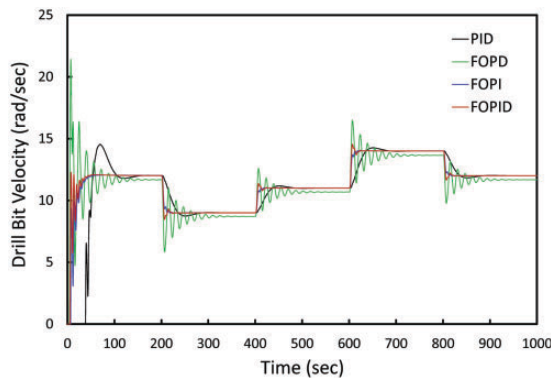


Figure 12. Drill bit velocities under variation in the reference velocity.

PID: proportional-integral-derivative; FOPD: fractional-order proportional-derivative; FOPI: fractional-order proportional-integral; FOPID: fractional-order proportional-integral-derivative.

Variations in the reference speed. The reference velocity value was modified every 200 s (12, 9, 11, 14, and 12 rad/s) to test the dynamic robustness of the proposed controllers. The WOB was kept constant at 100 kN to show only the effect of variation of reference velocity (see Figure 10).

Figure 11 shows the response of rotary table velocity resulting from the drillstring system with PID, FOPD, FOPI, and FOPID controllers. One can see that all controllers suppress the stick–slip vibration of the drillstring and track the reference velocity signal. The FOPD has a faster response with no overshoot, which can be

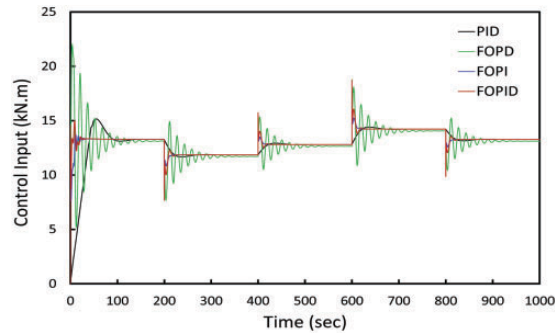


Figure 13. Control signals under variation in the reference velocity.

PID: proportional-integral-derivative; FOPD: fractional-order proportional-derivative; FOPI: fractional-order proportional-integral; FOPID: fractional-order proportional-integral-derivative.

explained by the absence of the integral parameter, which reduces the rise time in position control. The FOPD stabilized slightly under the reference velocity values. The FOPID shows a faster response time than the FOPI, which shows good performance compared with the PID.

Figure 12 shows the response of the drill bit velocity resulting from the controlled drillstring system with the proposed controllers. All controllers could suppress the stick–slip vibration of the drillstring at the drill bit and track the reference velocity signal. The FOPD has a slower response time with high oscillation. However, it is strongly affected by the variation of the reference velocity. The FOPID has a faster response time than the FOPI, which shows better performance than the PID.

Figure 13 shows the control signals of the proposed fractional-order controllers under variation in the reference velocity. The FOPD controller shows high oscillation with a higher overshoot. It has a slower response time, and it is strongly affected by variation in the reference velocity. The FOPID controller has a faster response time and high overshoot compared with the FOPI and PID. However, the FOPI controller has a slightly higher overshoot than the PID under the WOB variation.

Conclusion

The main focus of this work was to demonstrate the effectiveness of fractional-order controllers to suppress the stick–slip vibration of a drillstring system and to track the desired velocity under parameter variations. The simulation results confirmed that these goals were achieved using the FOPI, FOPD, and FOPID controllers. Although the FOPD's control was strongly sensitive to parameter variations and exhibited higher oscillations and slower response time, it ultimately tracked the reference velocity value. The FOPID shows better suppression performance, because of its additional DOF compared with the FOPI controller. For a similar reason, the FOPI had a faster response and improved stability than the traditional PID controller. Future work related to fractional-order controllers for active vibration control in drillstrings could include applying different tuning methods and adaptive and hybrid fractional-order controllers.


Declaration of conflicting interests

The author(s) declared no potential conflicts of interest with respect to the research, authorship, and/or publication of this article.

Funding

The author(s) disclosed receipt of the following financial support for the research, authorship, and/or publication of this article: This publication was made possible by an NPRP grant (NPRP10-0101-170081) from the Qatar National Research Fund (a member of Qatar Foundation).

ORCID iD

Mohamed Gharib  <https://orcid.org/0000-0003-2259-7576>

References

1. Lin W, Chávez JP, Liu Y, et al. Stick–slip suppression and speed tuning for a drill-string system via proportional-derivative control. *Appl Math Model* 2020; 82: 487–502.
2. Fu M, Zhang P, Li J, et al. Observer and reference governor based control strategy to suppress stick–slip vibrations in oil well drill-string. *J Sound Vib* 2019; 457: 37–50.
3. Zhang Q and Xv S. Stick–slip vibration suppression of drill string based on fractional order PID. In: *2019 international conference on computer network, electronic and automation (ICCNEA)*, 2019, pp.468–473. New York, NY: *IEEE*.
4. Tian J, Wei L, Yang L, et al. Research and experimental analysis of drill string dynamics characteristics and stick–slip reduction mechanism. *J Mech Sci Technol* 2020; 34: 977–986.
5. Saldívar B, Mondié S, Niculescu SI, et al. A control oriented guided tour in oilwell drilling vibration modeling. *Ann Rev Control* 2016; 42: 100–113.
6. Navarro-López EM and Cortés D. Sliding-mode control of a multi-DOF oilwell drillstring with stick–slip oscillations. In: *2007 American control conference*, 2007, pp.3837–3842. New York, NY: *IEEE*.
7. Challamel N. Rock destruction effect on the stability of a drilling structure. *J Sound Vib* 2000; 233: 235–254.
8. Vaziri V, Kapitaniak M and Wiercigroch M. Suppression of drill-string stick–slip vibration by sliding mode control: numerical and experimental studies. *Eur J Appl Math* 2018; 29: 805–825.
9. Rudat J, Dashevskiy D et al. Development of an innovative model-based stick/slip control system. In: *SPE/IADC drilling conference and exhibition*, 2011, pp.139996–MS. Amsterdam, The Netherlands: Society of Petroleum Engineers.
10. Qiu H, Yang J and Butt S. Investigation on bit stick–slip vibration with random friction coefficients. *J Petrol Sci Eng* 2018; 164: 127–139.
11. Lin YQ and Wang YH. Stick–slip vibration of drill strings. *J Eng Ind* 1991; 113: 38–43.
12. Canudas de Wit C, Rubio FR and Corchero MA. D-OSKIL: a new mechanism for controlling stick–slip oscillations in oil well drillstrings. *IEEE Trans Contr Syst Technol* 2008; 16: 1177–1191.
13. Zhu X, Tang L and Yang Q. A literature review of approaches for stick–slip vibration suppression in oilwell drillstring. *Adv Mech Eng* 2014; 6: 967952.
14. Pelfrene G, Sellami H, Gerbaud L, et al. (2011) Mitigating stick–slip in deep drilling based on optimization of PDC bit design. In: *SPE/IADC drilling conference and exhibition*, 2011, pp.139839–MS. Amsterdam, The Netherlands: Society of Petroleum Engineers.
15. Hu L, Palazzolo A and Karkoub M. Suppression of lateral and torsional stick–slip vibrations of drillstrings with impact and torsional dampers. *J Vib Acoust* 2016; 138.
16. Selnes KS, Clemmensen CC, Reimers N, et al. (2008) Drilling difficult formations efficiently with the use of an antistall tool. In: *IADC/SPE drilling conference*, 2008, pp.111874–MS. Amsterdam, The Netherlands: Society of Petroleum Engineers.
17. Jansen JD and Van Den Steen L. Active damping of self-excited torsional vibrations in oil well drillstrings. *J Sound Vib* 1995; 179: 647–668.
18. Dunayevsky V and Abbassian F. Application of stability approach to bit dynamics. *SPE Drill Completion* 1998; 13: 99–107.
19. Serrarens A, Van De Molengraaf M, Kok J, et al. *Hinf* control for suppressing stick–slip in oil well drillstrings. *IEEE Contr Syst Mag* 1998; 18: 19–30.
20. Yigit A and Christoforou A. Coupled torsional and bending vibrations of actively controlled drillstrings. *J Sound Vib* 2000; 234: 67–83.
21. Podlubny I. Fractional-order systems and fractional-order controllers. *Inst Exp Phys* 1994; 12: 1–18.
22. Monje CA, Vinagre BM, Feliu V, et al. Tuning and auto-tuning of fractional order controllers for industry applications. *Control Eng Pract* 2008; 16: 798–812.
23. Das S, Pan I, Das S, et al. Improved model reduction and tuning of fractional-order $pid\mu$ controllers for analytical rule extraction with genetic programming. *ISA Trans* 2012; 51: 237–261.
24. Zhao H, Deng W, Yang X, et al. An optimized fractional order PID controller for suppressing vibration of ac motor. *J Vibroeng* 2016; 18: 2205–2220.
25. Petráš I. Tuning and implementation methods for fractional-order controllers. *Fract Calc Appl Anal* 2012; 15: 282–303.
26. Loverro A. Fractional calculus: history, definitions and applications for the engineer. *Rapport Tech* 2004; 1–28.
27. Podlubny I. *Fractional differential equations: an introduction to fractional derivatives, fractional differential equations, to methods of their solution and some of their applications*. Amsterdam, The Netherlands: Elsevier, 1998.
28. Caputo M. Linear models of dissipation whose q is almost frequency independent-ii. *Geophys J Int* 1967; 13: 529–539.
29. Cafagna D. Fractional calculus: a mathematical tool from the past for present engineers [past and present]. *IEEE Ind Electron Mag* 2007; 1: 35–40.
30. Valério D and Da Costa JS. Introduction to single-input, single-output fractional control. *IET Control Theory Appl* 2011; 5: 1033–1057.
31. He JH and Ain QT. New promises and future challenges of fractal calculus: from two-scale thermodynamics to fractal variational principle. *Therm Sci* 2020; 24: 65.

32. Ain QT and He JH. On two-scale dimension and its applications. *Therm Sci* 2019; 23: 1707–1712.
33. He JH, Li ZB and Wang Q-l. A new fractional derivative and its application to explanation of polar bear hairs. *J King Saud Univ Sci* 2016; 28: 190–192.
34. He JH. A tutorial review on fractal spacetime and fractional calculus. *Int J Theor Phys* 2014; 53: 3698–3718.
35. Inc M. The approximate and exact solutions of the space-and time-fractional burgers equations with initial conditions by variational iteration method. *J Math Anal Appl* 2008; 345: 476–484.
36. Rashidi M, Domairry G, Doosthosseini A, et al. Explicit approximate solution of the coupled kdv equations by using the homotopy analysis method. *Int J Math Anal* 2008; 2: 581–589.
37. Oustaloup A, Levron F, Mathieu B, et al. Frequency-band complex noninteger differentiator: characterization and synthesis. *IEEE Trans Circuits Syst I* 2000; 47: 25–39.
38. Tajjudin M, Rahiman MHF, Arshad NM, et al. Robust fractional-order pi controller with Ziegler-Nichols rules. *World Acad Sci Eng Technol* 2013; 7: 1823–1830.
39. Oustaloup A, Moreau X and Nouillant M. The crone suspension. *Control Eng Pract* 1996; 4: 1101–1108.
40. Valério D and Da Costa JS. Tuning of fractional PID controllers with Ziegler–Nichols-type rules. *Signal Process* 2006; 86: 2771–2784.
41. Shah P and Agashe S. Review of fractional PID controller. *Mechatronics* 2016; 38: 29–41.
42. Tepljakov A, Petlenkov E and Belikov J. Fomcom: a MATLAB toolbox for fractional-order system identification and control. *Int Microelectron Comput Sci* 2011; 2: 51–62.